A Multiply Charged Tetracaine Derivative Blocks Cyclic Nucleotide-Gated Channels at Subnanomolar Concentrations†

Ambarish S. Ghatpande, Ramalinga Uma,‡ and Jeffrey W. Karpen*,‡

Department of Physiology and Biophysics, University of Colorado Health Sciences Center, Denver, Colorado 80262

Received October 1, 2002; Revised Manuscript Received December 4, 2002

ABSTRACT: Cyclic nucleotide-gated (CNG) ion channels are central participants in sensory transduction, generating the electrical response to light in retinal photoreceptors and to odorants in olfactory receptors. They are expressed in many other tissues where their specific roles in signaling remain unclear. As is true for many other ion channels, there is a paucity of specific blockers needed to dissect the contributions of these channels to cell signaling. CNG channels are members of the superfamily of voltage-gated ion channels, and the local anesthetic tetracaine is known to block CNG channels in a manner that resembles the block of voltage-gated Na^+ channels. The amine in local anesthetics interacts with the charged selectivity filter of Na^+ channels, while the aromatic ring gets stuck in the inner cavity and has hydrophobic interactions with the residues lining that region. Here we have synthesized a derivative of tetracaine, 3-[(aminopropyl)-amino]-*N*,*N*-dimethyl-*N*-(2-{[4-(butylamino)benzoyl]oxy}ethyl)propan-1-aminium acetate (APPA-tetracaine), that contains three positively charged amines at physiological pH instead of one. This compound blocked several different CNG channels in the picomolar to nanomolar concentration range at positive membrane potentials, making it several orders of magnitude more potent than tetracaine. In contrast, significant block of Na^+ channels by APPA-tetracaine required concentrations of hundreds of nanomolar. The results suggest that the highly charged moiety of APPA-tetracaine interacts strongly with the negative charge cluster in the selectivity filter of CNG channels. We propose that a variety of potent and specific ion channel blockers could be generated by expanding on traditional blocker structures to target the selectivity filters of other channels.

Cyclic nucleotide-gated (CNG[1]), cation-selective channels were first discovered in photoreceptor cells of the retina (*1*, *2*) where they generate a membrane hyperpolarization in response to a light-induced decrease in cGMP concentration (*3*). In olfactory receptor neurons, similar channels depolarize the plasma membrane following an odorant-induced increase in cAMP concentration (*4*). Although not voltage-activated, CNG channels belong to the superfamily of voltage-gated channels, in which each subunit or major domain contains six transmembrane helices and a pore region between the fifth and sixth helices (*5*, *6*). Retinal rod CNG channels are tetramers of CNGA1 and CNGB1 subunits (*7*−*10*), each of which carries a single cyclic nucleotide-binding site (*11*, *12*) and contributes to pore formation. Significant opening of the channel requires the binding of three molecules of cGMP (*7*), (*13*−*16*). Olfactory CNG channels are composed of at least 3 different pore-forming subunits CNGA2, CNGA4, and CNGB1 (*17*−*22*). CNGA1 and CNGA2 form homomeric channels when expressed on their own (*8*, *17*, *18*) and have been extensively studied as models for the basic properties of CNG channels.

Since their discovery in the retina, CNG channels have been found in many other tissues including heart, endothelium, skeletal muscle, liver, kidneys, testes, and several areas of the brain, though their exact roles in these tissues remain largely unknown. Our lack of knowledge of the functions of CNG channels in most tissues points to the need for specific pharmacological tools. In particular, a reversible, pore-blocking agent would be useful for investigating the physiological roles of cyclic nucleotide-induced changes in membrane potential and Ca^{2+} entry in various signaling pathways. The widely used CNG channel blocker L-*cis*-diltiazem (*23*, *24*) blocks CNG channels incompletely at micromolar concentrations and has multiple molecular targets. A recently discovered snake toxin may represent a promising beginning in that arena (*25*). Pseudechetoxin (PsTX) blocks homomeric CNGA2 channels at nanomolar concentrations; however, much higher concentrations are required to block homomeric CNGA1 channels and heteromeric rod and olfactory CNG channels.

Local anesthetics are well-known blockers of cation channels. For example, tetracaine (Figure 1) blocks Na^+, Ca^{2+}, and CNG channels (*26*−*29*). Many studies on local anesthetics and anti-arrhythmic drugs have suggested the existence of two distinct blocker-binding sites in voltage-gated Na^+ channels, one polar and the other hydrophobic in character. Site-directed mutagenesis studies point to the involvement of the selectivity filter in binding polar headgroups of channel blockers (*30*). Other studies indicate that

† Supported by National Institutes of Health Grant EY09275.

* Corresponding author. Telephone: 503-494-7463. Fax: 503-494-4352. E-mail: karpenj@ohsu.edu.

‡ Present address: Department of Physiology and Pharmacology, L334, Oregon Health & Science University, Portland, OR 97239.

[1] Abbreviations: CNG, cyclic nucleotide-gated; APPA-tetracaine, 3-[(aminopropyl)amino]-*N*,*N*-dimethyl-*N*-(2-{[4-(butylamino)benzoyl]-oxy}ethyl)propan-1-aminium acetate; CHO, Chinese hamster ovary.

10.1021/bi027031m CCC: $25.00 © 2003 American Chemical Society
Published on Web 12/21/2002

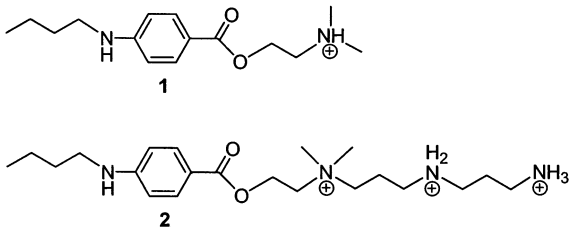

FIGURE 1: Structure of tetracaine (compound 1) and APPA-tetracaine (compound 2).

the hydrophobic binding site for local anesthetics may involve aromatic residues in the sixth transmembrane helices (S6) of at least two of the four major domains (*31*, *32*). In similar fashion, pore glutamate residues in CNG channels appear to form the polar binding site for tetracaine (*33*). It is important to note, however, that charged polyamines lacking aromatic groups block CNG channels at millimolar concentrations and permeate through the channel (*34*). Taken together, previous findings suggest that the aromatic moiety of tetracaine interacts with a hydrophobic binding site in the pore of CNG channels. Recent structural work on K^+ channels has revealed a pore architecture, containing a narrow selectivity filter and an inner cavity, that would support the binding of both hydrophilic and hydrophobic portions of a blocker (*35*, *36*).

Before molecular information on selectivity filters was available, it was difficult to design appropriate blockers. The negative charge cluster in the pore of CNG channels (four glutamates in homomeric channels, two or three in heteromeric channels (*37*−*39*)) and the low selectivity among cations suggested to us that multiply charged derivatives of tetracaine might fit in the pore and block these channels with high potency and specificity. We report here on one such derivative, in which two propylamino groups in tandem were attached to the tertiary amine of tetracaine. This compound contains three positive charges at physiological pH and blocks several different CNG channels with high affinity. Moreover, this blocker is selective for CNG channels over Na^+ channels and thus can complement available pharmacological tools to study CNG channel physiology.

MATERIALS AND METHODS

Synthesis and Purification of 3-[(Aminopropyl)amino]-N,N-dimethyl-N-(2-{[4-(butylamino)benzoyl]oxy}ethyl)propan-1-aminium acetate (APPA-tetracaine) (Compound 2). A mixture of tetracaine (compound 1) 2.5 g (9.46 mmol, Sigma-Aldrich) and 3-bromopropylamine hydrochloride 2.1 g (10 mmol, Sigma-Aldrich) in 20 mL ethanol was refluxed for 8 h. Reaction progress was followed by thin-layer chromatography on silica gel (0.2 mm), developed with 2-propanol/acetic acid/water (5:3:2), and visualized by UV shadowing. Analysis of the reaction mixture indicated the presence of two more polar spots in addition to some unreacted tetracaine. Removal of solvent in vacuo gave a residue that was purified by ion exchange HPLC (PolyCAT A, 21 × 250 mm, 5 μm, 300 Å, PolyLC) using a 5−500 mM ammonium acetate gradient (pH 5 with acetic acid). Unreacted tetracaine eluted first, the mono propylamino derivative, 3-amino-*N*,*N*-dimethyl-*N*-(2-{[4-(butylamino)benzoyl]oxy}ethyl)propan-1-aminium acetate, eluted second, followed by compound 2 in the ratio 67:27:6 (peak areas monitored at 312 nm). Compound 2 was further purified by RP-HPLC (Xterra Prep RP_8, 19 × 100 mm, 5 μm, Waters) using a water−methanol gradient (5 mM ammonium acetate, pH 5 with acetic acid, throughout) and dried repeatedly using a Speed-Vac (Savant).

NMR and mass spectrometry data for compound 2 were as follows: ^{1}H (500 MHz) NMR (CD_3OD) δ 7.79 (d, J = 9 Hz, $2H_f$), 6.60 (d, J = 9 Hz, $2H_e$), 4.88 (s, 4H, N*H*), 4.72 (br s, $2H_g$), 3.81 (br s, $2H_h$), 3.51−3.55 (m, $2H_j$), 3.23 (s, $6H_{i,i'}$), 3.15 (t, J = 7 Hz, $2H_d$), 3.01 (t, J = 6.5 Hz, $2H_m$), 2.78 (t, J = 6.5 Hz, $2H_o$), 2.75 (t, J = 6.5 Hz, $2H_l$), 2.05 (br s, $2H_k$), 1.91 (s, 3H, CH_3COO^-), 1.87 (br s, $2H_n$), 1.58−1.64 (m, $2H_c$), 1.41−1.48 (m, $2H_b$), 0.97 (t, J = 7 Hz, $3H_a$) ppm (peak assignments were aided by ^{1}H-^{1}H COSY experiment); ^{13}C (125 MHz) NMR (CD_3OD) δ 178.67 (CH_3COO^-), 167.68, 155.43, 132.91 (2C), 116.28, 112.28 (2C), 64.51, 64.11, 58.48, 52.32 (2C), 46.91, 46.34, 43.75, 38.70, 32.38, 26.78, 23.54 (CH_3COO^-), 22.42, 21.42, 14.36 ppm; a MALDI-TOF mass spectrum was acquired using α-cyano-4-hydroxycinnamic acid as the matrix, (M^+) calcd 379.31, found 379.31.

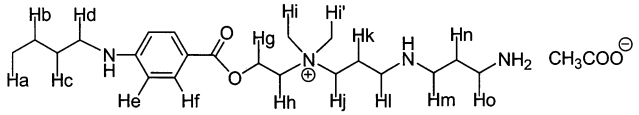

2

Channel Expression and Experimental Preparations. cRNAs encoding CNGA1 and CNGA2 were transcribed in vitro using the mMESSAGE mMACHINE T7 kit (Ambion, Austin, TX) and microinjected into *Xenopus* oocytes. Each oocyte was injected with 50 nl of mRNA at a concentration of 0.5 ng/nL. After injection, the oocytes were incubated at room-temperature overnight, 18 °C for 24 h and 16 °C thereafter. Electrophysiological recordings were made from excised, inside-out patches 2−10 days after injection.

Chinese hamster ovary (CHO) cells stably transfected with the RIIA rat brain Na^+ channel gene were maintained in 10 mL MEM (Life Technologies) supplemented with 5% v/v fetal bovine serum (Gemini), 2% w/v sodium bicarbonate (Sigma-Aldrich), 0.2 mg/mL antibiotic G418 (Life Technologies) and grown in 75 cm^2 flasks at 37 °C in a humidified atmosphere with 5% CO_2. Cells plated in 100 mm culture dishes were washed with phosphate-buffered saline, treated with a 0.3% trypsin-EDTA solution in saline to detach them, suspended in serum-containing medium, and used in whole-cell patch clamp recording.

Rod outer segments containing native CNG channels were obtained from the retinas of light-adapted frogs, *Rana pipiens*. The retinas were removed and placed in Ringers solution containing the following (mM): 111 NaCl, 2.5 KCl, 1 $CaCl_2$, 1 $MgCl_2$, 10 D-glucose, 3 HEPES (pH 7.5), and 0.02 EDTA. The retinas were chopped into small pieces and stored at 16 °C. For recording, a small piece of retina was finely chopped with a razor blade in a small amount of Ringers solution. The cell suspension was added to the recording chamber; the floor was made sticky by prior filling with 1 mg/mL poly-L-lysine hydrobromide (30 000−70 000 mol wt; Sigma-Aldrich). The chamber was then rinsed thoroughly with Ringers solution to remove debris and cells

that were not stuck. Inside-out patches were excised from isolated rod outer segments in visible light.

Electrophysiology. Patch clamp recordings were done at room temperature using an Axopatch 1D amplifier (Axon Instruments, Foster City, CA). Electrodes were pulled from borosilicate glass and heat polished; the resistances were 0.5−1.5 MΩ (excised oocyte patches), 1.2−2.5 MΩ (whole-cell), and 2−5 MΩ (excised rod outer segment patches). Seal resistances were typically 2−20 GΩ. Currents were low-pass filtered with an eight-pole Bessel filter and sampled at five times the filter frequency. For CNG channel experiments in excised patches, leak currents in the absence of cGMP were subtracted from all records. For Na^+ channel experiments in whole-cell mode, the pipet was back-filled with APPA-tetracaine in intracellular solution. The tip of the pipet was front-filled with a tiny amount of APPA-tetracaine-free intracellular solution. This allowed a current−voltage relation in the absence of APPA-tetracaine to be recorded shortly after break-in. Leak subtraction was done using eight subpulses in the hyperpolarizing direction after each depolarizing pulse. Capacitance compensation and correction for series resistance (80% correction) were applied using the built-in circuitry of the amplifier. Solutions were applied to excised patches with an RSC-100 rapid solution changer (Molecular Kinetics, Pullman, WA). For oocyte patch recordings, the extracellular and control intracellular solutions contained the following (mM): 130 mM NaCl, 0.02 EDTA, 1 EGTA, and 2 HEPES (pH 7.6). For whole-cell recording from CHO cells, the extracellular and intracellular solutions contained the following (mM): 130 NaCl, 4 KCl, 1.5 $CaCl_2$, 1.5 $MgCl_2$, 5 D-glucose, 20 sucrose, and 5 HEPES (pH 7.4). Rod outer segment patches were excised in the same solution used for CHO cells; subsequently the bath chamber was perfused with a solution (used also as the extracellular solution) containing the following (mM): 111 NaCl, 2.5 KCl, 4 EDTA, 3 HEPES (pH 7.5). APPA-tetracaine was dissolved in water to make a 10 μM solution, which was further diluted to 200 nM and stored frozen in aliquots. Required dilutions were made from this working stock using appropriate intracellular solutions.

RESULTS

The structures of tetracaine and APPA-tetracaine are shown in Figure 1. Both molecules are protonated at physiological pH and carry charges of +1 and +3, respectively. We studied APPA-tetracaine block of expressed homomeric channels containing CNGA1 or CNGA2 subunits and native heteromeric CNG channels from retinal rod outer segments. Figure 2A shows that APPA-tetracaine is an extremely potent blocker of CNGA1 channels. In two different patches (superimposed), 100 pM APPA-tetracaine blocked 66% and 200 pM blocked 97% of the current through CNGA1 channels activated by saturating cGMP (1 mM) at +40 mV. The apparent K_D at +40 mV in seven patches averaged 30 pM, with some patch-to-patch variability (Table 1). APPA-tetracaine was 7500-fold more potent than tetracaine in blocking CNGA1 channels at +40 mV and 120-fold more potent at 0 mV (Table 1). The block is even more potent at 50 μM cGMP, which is closer to a physiological concentration. The APPA-tetracaine concentrations used in Figure 2A completely block the current at +40 mV (not shown). Steady-state block is achieved very slowly at lower concentrations, and the long positive holding potentials usually break patches. The block by APPA-tetracaine is strongly voltage-dependent, and we have taken advantage of this, using higher concentrations of APPA-tetracaine to study the efficiency of block at the lower cGMP concentration. Figure 2B shows the block by 200 nM APPA-tetracaine of inward current at −50 mV induced by 50 μM cGMP. The calculated K_D from these and other data was 28 nM at this potential. If the voltage dependence of block is similar

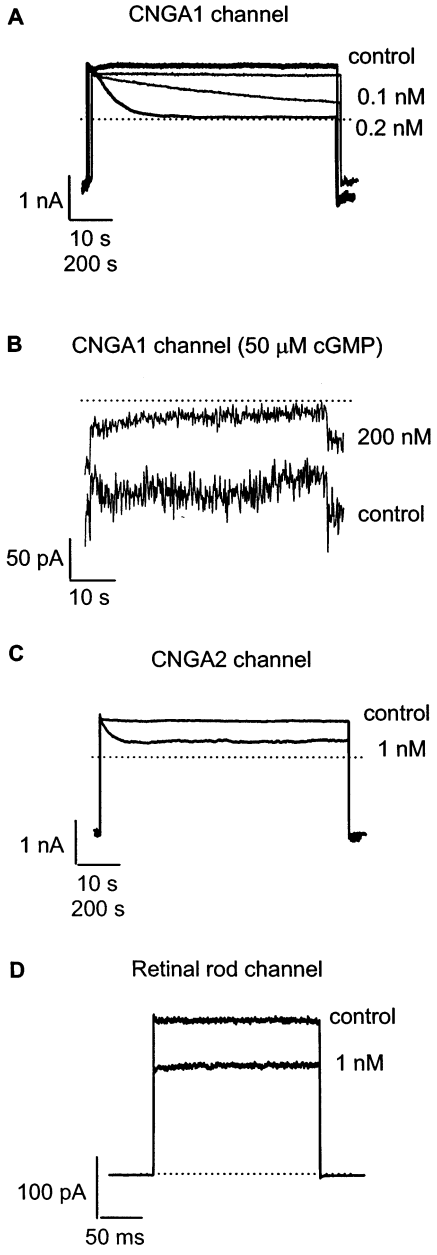

FIGURE 2: APPA-tetracaine block of CNGA1, CNGA2 and native CNG channels. Expressed CNGA1 (A and B) and CNGA2 (C) channels were studied in excised oocyte patches, and native rod channels (D) were studied in excised rod outer segment patches. Currents were activated by 1 mM (A, C, D) and 50 μM (B) cGMP applied to the cytoplasmic surface. Holding and test potentials were −80 and +40 mV (A and C), −80 and −50 mV (B), and 0 and +50 mV (D). The time calibration bar in A and C represents 10 and 200 s for each "control" and experimental current trace. Dotted lines show zero current level. Data in panel A are from two different patches: thin (control and 0.1 nM) and thick traces (control and 0.2 nM).The sampling rates were 250 Hz for 60 s voltage pulses, 10 Hz for 20 min pulses, and 5 kHz for 200 ms pulses.

Table 1. Block of CNG Channels by APPA-Tetracaine and Tetracaine[a]

channel	$K_{D\,(40,H)}$ (nM)	$k_{on(40,H)}$ ($\times 10^7$, $M^{-1}\,s^{-1}$)	$k_{off(40,H)}$ ($\times 10^{-4}$, s^{-1})	$K_{D(0,H)}$ (nM)	$z\delta$	$K_{D(-50,L)}$ (nM)
			APPA-Tetracaine			
CNGA1	0.03 ± 0.02 (7)	1.69 ± 2.0 (4)	2.28 ± 1.1 (4)	6.9 ± 4.7 (5)	2.6 ± 0.3	28 (1)[b]
CNGA2	0.9 ± 0.06 (10)	1 ± 0.5 (4)	80 ± 20 (4)	148 (1)	3.0	–
ROS	4 ± 2.9 (3)	–	–	–	–	–
			Tetracaine			
CNGA1	230 ± 200 (4)	–	–	800 ± 700 (4)	0.8 ± 0.1	–

[a] Numbers in subscripts indicate potential (in mV) at which experiment was done, except for rod outer segment (ROS) experiments that were done at +50 mV; subscripts H and L indicate experiments done at 1 mM and 50 μM cGMP. K_D is the apparent dissociation constant calculated from the relation: $I_{+D}/I_{-D} = K_D/(K_D + [D])$, where the left side is the current in the presence of the blocker divided by the current in its absence and [D] is the blocker concentration. Values are shown as mean ± S.D., and the number of independent experiments is indicated in parentheses. The association and dissociation rate constants, k_{on} and k_{off}, were calculated from the following equations: $1/\tau = k_{on}[D] + k_{off}$, and $K_D = k_{off}/k_{on}$; τ was determined from monoexponential fits to the data. $K_{D(0)}$, the apparent dissociation constant at 0 mV, and $z\delta$, the effective valence of the blocker were determined from fits to the Woodhull eq (*26*): $I_{+D}/I_{-D} = K_{D(0)}\, e^{(-z\delta FV/RT)}/\{K_{D(0)}\, e^{(-z\delta FV/RT)} + [D]\}$; all other symbols have their usual meaning. [b] Similar results were obtained at low cGMP on three other patches; the ratios of the currents at low and high cGMP were slightly different among the four patches.

at high and low cGMP (see below), the K_D at +40 mV would be approximately 3 pM at 50 μM cGMP (consistent with the complete block observed at 100 pM). The higher efficacy of block by APPA-tetracaine at low versus high cGMP concentrations indicates that APPA-tetracaine blocks closed channels with higher affinity than open channels, in agreement with earlier findings on tetracaine (*29*, *33*). APPA-tetracaine is also a potent blocker of CNGA2 channels, although the apparent affinity is not as high as for CNGA1 channels. In Figure 2C, 1 nM blocked ~50% of the current through CNGA2 channels at saturating cGMP. Figure 2D shows data from a rod outer segment patch, in which 1 nM APPA tetracaine blocked 30% of the current through native CNG channels activated by saturating cGMP. Rod outer segment patches broke while attempting to record the voltage protocol shown in Figure 2A−C; therefore, rod outer segment patches were subjected to a series of voltage pulses to +50 mV until steady-state block had been reached (judged by chart record), and the current remaining at +50 mV was recorded. Table 1 compares APPA-tetracaine block of CNGA1, CNGA2, and rod CNG channels, from several experiments at different concentrations of APPA-tetracaine. At positive potentials and saturating cGMP, the estimated K_D's were 30 pM, 900 pM, and 4 nM, respectively.

The time courses of block in panels A (thick trace) and C of Figure 2 were fit as single exponential decays with time constants of 103 and 35.8 s, respectively. The calculated bimolecular rate constants are 4.8×10^7 and 1.6×10^7 M^{-1} s^{-1} for block of CNGA1 and CNGA2 channels (see Table 1 for equations used). The similar on-rates of block suggest that the 30-fold higher affinity of APPA-tetracaine for CNGA1 channels derives in large part from a longer dwell time of the drug in the channel.

Given the charged nature of APPA-tetracaine, we tested the membrane potential dependence of its block of homomeric channels, as shown in Figure 3. APPA-tetracaine block of CNGA1 and CNGA2 channels was highly potential-dependent, and a fit of the Woodhull model ((*26*), see Table 1 for equation) to the data gives K_D values at 0 mV of 3 and 148 nM for CNGA1 and CNGA2 channels. The corresponding 'effective valence' or $z\delta$ values are 2.4 and 3.0. This parameter is generally taken to mean the valence of the blocker (z) multiplied by the fractional electrical distance of the membrane electric field traversed by the blocker (δ).

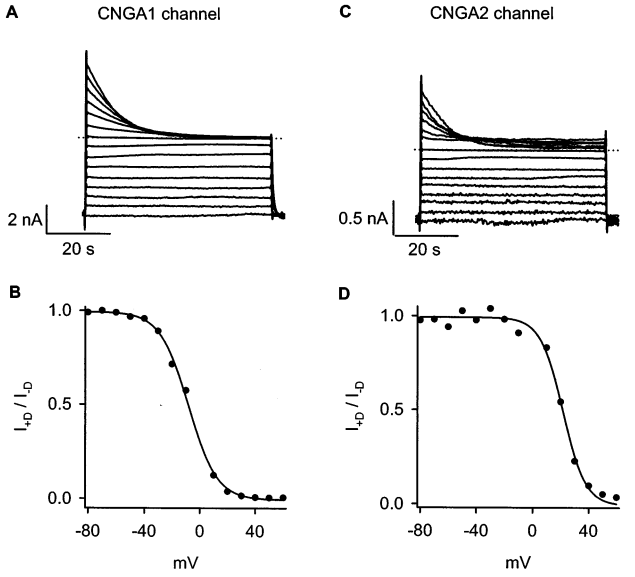

FIGURE 3: APPA-tetracaine block of homomeric CNGA1 and CNGA2 channels is highly potential-dependent. Excised patches from oocytes expressing CNGA1 (A) or CNGA2 (C) were subjected to a series of depolarizing pulses from −80 to +60 mV (10 mV increments) in the presence of 1 mM cGMP and 10 nM APPA-tetracaine (sampling frequency was 100 Hz; inter-pulse interval was 142 s, to allow complete recovery from block). Panels B and D show plots of the ratio of current in the presence and absence of blocker at each potential (except 0 mV). Values obtained from fits to the Woodhull equation (Table 1) were $K_{D(0)} = 3.1$ nM, $z\delta = 2.6$; and $K_{D(0)} = 148$ nM, $z\delta = 3.0$ for data in panels B and D.

These $z\delta$ values suggest that all three positively charged amines contribute to block and that they cross most of the membrane electric field from the inside to reach their blocking site(s). Consistent with this, the $z\delta$ value for tetracaine block was 0.8 (Table 1) about one-third the value for APPA-tetracaine.

Finally, we tested the ability of APPA-tetracaine to block rat brain Na^+ channels, as shown in Figure 4. The patch pipet was filled with 20 nM APPA-tetracaine, and whole-cell current−voltage relations were recorded every 20 s. Figure 4A shows control traces recorded immediately after going whole-cell, before APPA-tetracaine was able to diffuse into the cell (the pipet was front-filled with a tiny amount of APPA-tetracaine-free solution). In Figure 4B, current traces at +40 mV from six such consecutive protocols recorded

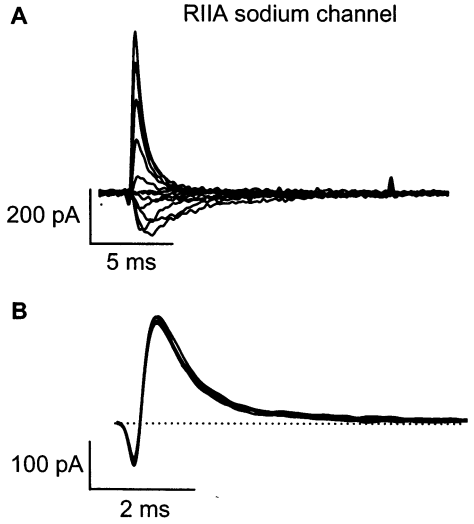

FIGURE 4: APPA-tetracaine does not block voltage-sensitive rat brain Na^+ channels at 20 nM concentration. Whole-cell current−voltage relations were recorded from CHO cells stably expressing the RIIA Na^+ channel, in the presence of 20 nM intracellular APPA-tetracaine. Twelve depolarizing pulses of 15 ms duration (sampling frequency of 16.6 kHz) from −60 to +50 mV (10 mV increments) were applied from a holding potential of −70 mV. Before each depolarizing pulse, a brief hyperpolarizing pulse to −90 mV was applied for 6 ms. (A) I−V recorded immediately after going whole-cell (see Materials and Methods). (B) Six current traces at +40 mV, from consecutive I−Vs after 15 min of internal perfusion with 20 nM APPA-tetracaine (same cell as A).

after 15 min of perfusion are shown. No significant block was observed, as indicated by the superimposed traces. In other experiments, 200 nM APPA-tetracaine caused less than 50% block of Na^+ currents (not shown). The data indicate that approximately 100-fold higher concentrations of APPA-tetracaine are required to block Na^+ currents than currents through native rod CNG channels at saturating cGMP. This factor is likely to be much larger at physiological cGMP concentrations, based on the results in Figure 2B. Thus, APPA-tetracaine appears to be a selective blocker of CNG channels over Na^+ channels.

DISCUSSION

We have synthesized a charged derivative of tetracaine containing a multivalent, positively charged headgroup and a hydrophobic tail that blocks CNG channels. Addition of the charged headgroup results in a vast gain in apparent affinity (almost 4 orders of magnitude at positive potentials) over the parent compound tetracaine.

The widely used pharmacological agent L-*cis*-diltiazem blocks native CNG channels with micromolar affinity from the cytoplasmic side and millimolar affinity from the extracellular side. L-*cis*-Diltiazem is not specific and has been shown to block both Na^+ and Ca^{2+} channels (*40*, *41*). Similarly, other reagents currently in use, tetracaine (*26*), pimozide (*42*), and LY-83,583 (*43*), block CNG channels in the micromolar range and are not specific. In contrast, APPA-tetracaine blocks CNG channels in the subnanomolar range and shows specificity over Na^+ channels. Thus, it should serve as a useful pharmacological tool in the study of CNG channel physiology and biophysics. APPA-tetracaine does not cross cell membranes because of its highly charged nature (data not shown); as such, it must be introduced into cells by whole-cell patch-clamp techniques or microinjection.

The molecular basis for the extremely potent block by APPA-tetracaine remains to be fully explored, but two explanations are apparent from the current study and earlier work. First, an intrinsically high affinity of APPA-tetracaine for the pore (monitored at 0 mV) probably results from the interaction of the three positive charges with the negatively charged glutamate residues that line the pore. The apparent difference in affinity of APPA-tetracaine for CNGA1 homomeric channels (30 pM) and native rod outer segment channels (4 nM) at 1 mM cGMP supports this hypothesis. The pore of native rod outer segment channels probably contains two or three glutamates (*37*−*39*), as opposed to four glutamates in the homomeric CNGA1 pore. Fodor et al. also presented evidence that tetracaine interacts with the pore glutamate residues (*33*). Second, APPA-tetracaine is driven into the pore at positive potentials, resulting in an even higher apparent affinity. The potential dependence of block suggests that at least two of the three charges completely traverse the membrane electric field, assuming the simple Woodhull model (Table 1) applies. Given the known permeant block by polyamines of CNG channels (*34*), it is tempting to speculate that the propylamino groups of APPA-tetracaine interact with the pore glutamates, and perhaps make it past them. The aromatic moiety gets stuck and prevents the compound from passing through the channel completely.

APPA-tetracaine block is state-dependent, apparently blocking closed channels much more strongly than open channels. A similar finding was reported earlier for tetracaine (*33*). This may explain the difference in block of CNGA1 and CNGA2 channels (30 vs 900 pM). The 30-fold difference is similar to a 37-fold difference reported earlier for tetracaine block of these two channels (*33*). At saturating cGMP, CNGA1 channels are closed a much higher fraction of the time than CNGA2 channels (5% vs ≪1%). However, other differences between the two channels may contribute to the difference in affinity.

One of our objectives in synthesizing APPA-tetracaine was to exploit the differences between related cation channel pores to achieve specificity. APPA-tetracaine is selective for CNG channels over brain Na^+ channels. The highly charged moiety of APPA-tetracaine likely interacts more strongly with the selectivity filter of CNG channels, which contains two to four glutamates, than the selectivity filter of Na^+ channels, which contains aspartate, glutamate, and lysine (*44*). In effect, we have expanded on a basic blocker structure and purposely targeted the selectivity filter. Using this strategy in combination with emerging structural information (*45*), it should be possible to design potent and selective blockers of various therapeutically important targets such as Na^+ and Ca^{2+} channels.

ACKNOWLEDGMENT

We thank Dr. R. Lane Brown for helpful discussions and comments on the manuscript, Dr. Yiannis Koutalos, Dr. Chunhe Chen, and Silvio Rizzoli for help with rod outer segment preparation, Dr. S. Rock Levinson for advice on Na^+ channel experiments, Dr. David Jones and Dr. Joseph Zirrolli of the NMR and Mass Spectrometry Core Facilities of the University of Colorado Health Sciences Center, and Xuan Le for technical assistance.

REFERENCES

1. Fesenko, E. E., Kolesnikov, S. S. and Lyubarsky, A. L. (1985) *Nature 313*, 310−313.
2. Yau, K. W., and Baylor, D. A. (1989) *Annu. Rev. Neurosci. 12*, 289−327.
3. Pugh, E. N., Jr and Lamb, T. D. (1993) *Biochim. Biophys. Acta 1141*, 111−149.
4. Nakamura, T. and Gold, G. H. (1987) *Nature 325*, 442−444.
5. Heginbotham, L., Abramson, T. and MacKinnon, R. (1992) *Science 258*, 1152−1155.
6. Henn, D. K., Baumann, A. and Kaupp, U. B. (1995) *Proc. Natl. Acad. Sci. U.S.A. 92*, 7425−7429.
7. Cook, N. J., Hanke, W. and Kaupp, U. B. (1987) *Proc. Natl. Acad. Sci. U.S.A. 84*, 585−589.
8. Kaupp, U. B., Niidome, T., Tanabe, T., Terada, S., Bönigk, W., Stühmer, W., Cook, N. J., Kangawa, K., Matsuo, H., Hirose, T. et al. (1989) *Nature 342*, 762−766.
9. Chen, T. Y., Peng, Y. W., Dhallan, R. S., Ahamed, B., Reed, R. R. and Yau, K. W. (1993) *Nature 362*, 764−767.
10. Körschen, H. G., Illing, M., Seifert, R., Sesti, F., Williams, A., Gotzes, S., Colville, C., Müller, F., Dose, A., Godde, M., Molday, L., Kaupp, U. B. and Molday, R. S. (1995) *Neuron 15*, 627−636.
11. Brown, R. L., Gerber, W. V. and Karpen, J. W. (1993) *Proc. Natl. Acad. Sci. U.S.A. 90*, 5369−5373.
12. Brown, R. L., Gramling, R., Bert, R. J. and Karpen, J. W. (1995) *Biochemistry 34*, 8365−8370.
13. Haynes, L. W., Kay, A. R. and Yau, K. W. (1986) *Nature 321*, 66−70.
14. Zimmerman, A. L. and Baylor, D. A. (1986) *Nature 321*, 70−72.
15. Ruiz, M. L. and Karpen, J. W. (1997) *Nature 389*, 389−392.
16. Ruiz, M., Brown, R. L., He, Y., Haley, T. L. and Karpen, J. W. (1999) *Biochemistry 38*, 10642−10648.
17. Dhallan, R. S., Yau, K. W., Schrader, K. A. and Reed, R. R. (1990) *Nature 347*, 184−187.
18. Ludwig, J., Margalit, T., Eismann, E., Lancet, D. and Kaupp, U. B. (1990) *FEBS Lett. 270*, 24−29.
19. Liman, E. R. and Buck, L. B. (1994) *Neuron 13*, 611−621.
20. Bradley, J., Li, J., Davidson, N., Lester, H. A. and Zinn, K. (1994) *Proc. Natl. Acad. Sci. U.S.A. 91*, 8890−8894.
21. Sautter, A., Zong, X., Hofmann, F. and Biel, M. (1998) *Proc. Natl. Acad. Sci. U.S.A. 95*, 4696−4701.
22. Bönigk, W., Bradley, J., Müller, F., Sesti, F., Boekhoff, I., Ronnett, G. V., Kaupp, U. B. and Frings, S. (1999) *J. Neurosci. 19*, 5332−5347.
23. Stern, J. H., Kaupp, U. B. and MacLeish, P. R. (1986) *Proc. Natl. Acad. Sci. U.S.A. 83*, 1163−1167.
24. Haynes, L. W. (1992) *J. Gen. Physiol. 100*, 783−801.
25. Brown, R. L., Haley, T. L., West, K. A. and Crabb, J. W. (1999) *Proc. Natl. Acad. Sci. U.S.A. 96*, 754−759.
26. Hille, B. (2001) *Ion Channels of Excitable Membranes*, 3rd ed., Sinauer Associates, Sunderland, MA.
27. Palade, P. T. and Almers, W. (1985) *Pflugers Arch. 405*, 91−101.
28. Schnetkamp, P. P. (1990) *J. Gen. Physiol. 96*, 517−534.
29. Fodor, A. A., Gordon, S. E. and Zagotta, W. N. (1997) *J. Gen. Physiol. 109*, 3−14.
30. Sunami, A., Dudley, S. C., Jr. and Fozzard, H. A. (1997) *Proc. Natl. Acad. Sci. U.S.A. 94*, 14126−14131.
31. Ragsdale, D. S., McPhee, J. C., Scheuer, T. and Catterall, W. A. (1994) *Science 265*, 1724−1728.
32. Ragsdale, D. S., McPhee, J. C., Scheuer, T. and Catterall, W. A. (1996) *Proc. Natl. Acad. Sci. U.S.A. 93*, 9270−9275.
33. Fodor, A. A., Black, K. D. and Zagotta, W. N. (1997) *J. Gen. Physiol. 110*, 591−600.
34. Guo, D. and Lu, Z. (2000) *J. Gen. Physiol. 115*, 783−798.
35. Doyle, D. A., Morais Cabral, J., Pfuetzner, R. A., Kuo, A., Gulbis, J. M., Cohen, S. L., Chait, B. T. and MacKinnon, R. (1998) *Science 280*, 69−77.
36. Zhou, M., Morais-Cabral, J. H., Mann, S. and MacKinnon, R. (2001) *Nature 411*, 657−661.
37. He, Y., Ruiz, M. and Karpen, J. W. (2000) *Proc. Natl. Acad. Sci. U.S.A. 97*, 895−900.
38. Shammat, I. M. and Gordon, S. E. (1999) *Neuron 23*, 809−819.
39. Zhong, H., Molday, L. L., Molday, R. S. and Yau, K. W. (2002) *Nature 420*, 193−198.
40. Hashimoto, Y., Yabana, H. and Murata, S. (2000) *Eur. J. Pharmacol. 391*, 217−223.
41. Bohle, T. (1992) *J. Physiol. 445*, 303−318.
42. Nicol, G. D. (1993) *J. Pharmacol. Exp. Ther. 265*, 626−632.
43. Leinders-Zufall, T. and Zufall, F. (1995) *J. Neurophysiol. 74*, 2759−2762.
44. Heinemann, S. H., Terlau, H., Stühmer, W., Imoto, K. and Numa, S. (1992) *Nature 356*, 441−443.
45. Zhou, Y., Morais-Cabral, J. H., Kaufman, A. and MacKinnon, R. (2001) *Nature 414*, 43−48.

BI027031M